

# RESEARCH



Report No. UT-25.02

## SNOW PLOW PERFORMANCE MEASURES IN NON-RWIS LOCATIONS

**Prepared For:**

Utah Department of Transportation  
Research & Innovation Division

**Final Report  
August 2024**

## **DISCLAIMER**

The authors alone are responsible for the preparation and accuracy of the information, data, analysis, discussions, recommendations, and conclusions presented herein. The contents do not necessarily reflect the views, opinions, endorsements, or policies of the Utah Department of Transportation or the U.S. Department of Transportation. The Utah Department of Transportation makes no representation or warranty of any kind, and assumes no liability therefore.

## **ACKNOWLEDGMENTS**

The authors acknowledge the Utah Department of Transportation (UDOT) for funding this research, and the following individuals from UDOT on the Technical Advisory Committee for helping to guide the research:

- Ryan Ferrin
- David Stevens
- Brad Loveless
- Cody Oppermaun
- Jeff Williams
- Tyron McQuiddy
- Sean Berry
- Christopher Siavrakas
- John Sharp
- Matt Lazanich

## TECHNICAL REPORT ABSTRACT

1. Report No. UT-25.02		2. Government Accession No. N/A		3. Recipient's Catalog No. N/A	
4. Title and Subtitle Snow Plow Performance Measures in Non-RWIS Locations				5. Report Date August 2024	
				6. Performing Organization Code N/A	
7. Author(s) Gang Jiang, Biao Kuang, Zhenhua Shi, Zhihao Ma, Jianli Chen				8. Performing Organization Report No. N/A	
9. Performing Organization Name and Address University of Utah Department of Civil & Environmental Engineering 110 Central Campus Drive, Suite 2000 Salt Lake City, UT 84112				10. Work Unit No. 5H092 27H	
				11. Contract or Grant No. 24-8342	
12. Sponsoring Agency Name and Address Utah Department of Transportation 4501 South 2700 West P.O. Box 148410 Salt Lake City, UT 84114-8410				13. Type of Report & Period Covered Final Report September 2023 to August 2024	
				14. Sponsoring Agency Code PIC No. UT23.204	
15. Supplementary Notes Prepared in cooperation with the Utah Department of Transportation and the U.S. Department of Transportation, Federal Highway Administration					
16. Abstract <p>This project aims to enhance traffic safety by developing an Artificial Intelligence (AI) model and the weather interpolation method to evaluate snow cover conditions on road surfaces using existing roadside Closed-Circuit Television system (CCTV) images in non-Road Weather Information System (RWIS) locations. Snow-cover significantly impacts traffic safety, contributing to 24 percent of annual weather-related vehicle crashes. In Utah, where snow seasons can last up to seven months with over 25 winter storms annually, understanding snow-cover condition in real time is crucial for effective snow plow management by the Utah Department of Transportation (UDOT) and for public safety. Traditional methods for assessing road conditions rely on RWIS, which has limited coverage. The project will utilize image data from CCTV cameras to train a deep learning-based AI model for automatic evaluation of snow-cover condition. The methodology includes processing images to create labeled datasets, developing AI models based on AlexNet as the deep learning algorithms, and implementing these models to analyze real-time snow-cover conditions. Additionally, a weather interpolation method is developed to estimate real-time weather status in non-RWIS areas. The validation results show that our developed AI model can achieve over 97 percent accuracy in identifying various snow-cover states, including clear, partial snow, and full snow conditions. Furthermore, the developed weather interpolation method can provide a detailed view of the spatial distribution of air temperature, relative humidity, wind speed, precipitation, and snow accumulation. By leveraging existing CCTV networks, this project offers a cost-effective solution for large-scale, real-time road condition monitoring, closing information gaps, and enhancing winter road safety management.</p>					
17. Key Words Image recognition; Deep learning; Artificial intelligence (AI), Transportation assets; Snow cover evaluation; Weather interpolation; Road safety management		18. Distribution Statement Not restricted. Available through: UDOT Research & Innovation Div. 4501 South 2700 West P.O. Box 148410 Salt Lake City, UT 84114-8410 <a href="http://www.udot.utah.gov/go/research">www.udot.utah.gov/go/research</a>		23. Registrant's Seal N/A	
19. Security Classification (of this report)  Unclassified	20. Security Classification (of this page)  Unclassified	21. No. of Pages  47	22. Price  N/A		

## TABLE OF CONTENTS

LIST OF TABLES .....	v
LIST OF FIGURES .....	vi
UNIT CONVERSION FACTORS .....	vii
LIST OF ACRONYMS .....	viii
EXECUTIVE SUMMARY .....	1
1.0 INTRODUCTION .....	3
1.1 Problem Statement.....	3
1.2 Research Objectives.....	3
1.3 Research Scope .....	4
1.4 Outline of Report .....	4
2.0 LITERATURE REVIEW .....	5
2.1 Data Collection and Processing .....	5
2.1.1 Data Augmentation .....	5
2.1.2 Summer-to-Winter Image Translation Using GANs .....	6
2.1.3 Super Resolution .....	7
2.1.4 Brief Summary .....	8
2.2 Road Surface Condition Recognition AI Models .....	9
2.2.1 Artificial Intelligence Models .....	9
2.2.2 Applications of AI Models in Road Surface Condition Detection .....	10
2.2.3 Weather Interpolation .....	11
2.2.4 Brief Summary .....	12
3.0 METHODOLOGY .....	13
3.1 Research Process Overview .....	13
3.2 Data Collection and Processing .....	13
3.3 Data Annotations .....	16
3.4 Training of AlexNet as the Deep Learning Algorithm for Automated Road Condition Evaluation .....	17
3.4.1 Preparation of Training and Test Datasets.....	17
3.4.2 Model Architecture: AlexNet.....	17

3.4.3 Training Process.....	17
3.5 Accuracy Metrics.....	18
3.6 Weather Interpolation.....	19
3.6.1 Data Collection.....	19
3.6.2 Radial Basis Function (RBF) Interpolation.....	21
4.0 AI MODEL DEVELOPMENT.....	23
4.1 Performance of the Developed AI Model.....	23
4.2 Weather Interpolation.....	29
5.0 CONCLUSIONS.....	32
5.1 Summary.....	32
5.2 Findings.....	32
5.3 Limitations and Future Work.....	32
6.0 IMPLEMENTATION AND RECOMMENDATIONS.....	34
REFERENCES.....	35

## LIST OF TABLES

Table 1 Summary statistics of the image datasets .....	16
Table 2 Weather variables and regions of stations .....	20
Table 3 Classification performance metrics for the test dataset .....	24

## LIST OF FIGURES

Figure 1 Data augmentation example .....	6
Figure 2 Examples of GANs result (Mingjian Wu et al., 2023).....	7
Figure 3 Example of super resolution.....	8
Figure 4 The structure of SRGAN .....	8
Figure 5 Flowchart of Model Development and Improvement .....	13
Figure 6 The Filezilla Interface.....	14
Figure 7 100+ RWIS sites.....	15
Figure 8 Processing techniques (a) super resolution (b) logo inpainting.....	15
Figure 9 Sample image of road conditions .....	16
Figure 10 Regions and stations for weather data collection .....	21
Figure 11 Training and validation accuracy history over epochs .....	23
Figure 12 Confusion matrix for the test dataset.....	24
Figure 13 Success classified clear category images .....	25
Figure 14 Misclassify clear category as partial snow-cover category .....	25
Figure 15 Success classified partial snow-cover category images .....	26
Figure 16 Misclassify partial snow-cover category as clear category .....	27
Figure 17 Misclassify partial snow-cover category as full snow-cover category.....	27
Figure 18 Success classified full snow-cover category images .....	28
Figure 19 Misclassify full snow-cover category as clear category.....	28
Figure 20 Misclassify full snow-cover category as partial snow-cover category.....	29
Figure 21 Weather interpolation in Salt Lake City. (a) Temperature (b) Relative humidity (c) Wind speed (d) Precipitation accumulation within 24 hours.....	30
Figure 22 Interpolation of snow accumulation within 24 hours in Northern Utah.....	31

## UNIT CONVERSION FACTORS

<b>SI* (MODERN METRIC) CONVERSION FACTORS</b>				
<b>APPROXIMATE CONVERSIONS TO SI UNITS</b>				
Symbol	When You Know	Multiply By	To Find	Symbol
<b>LENGTH</b>				
in	inches	25.4	millimeters	mm
ft	feet	0.305	meters	m
yd	yards	0.914	meters	m
mi	miles	1.61	kilometers	km
<b>AREA</b>				
in <sup>2</sup>	square inches	645.2	square millimeters	mm <sup>2</sup>
ft <sup>2</sup>	square feet	0.093	square meters	m <sup>2</sup>
yd <sup>2</sup>	square yard	0.836	square meters	m <sup>2</sup>
ac	acres	0.405	hectares	ha
mi <sup>2</sup>	square miles	2.59	square kilometers	km <sup>2</sup>
<b>VOLUME</b>				
fl oz	fluid ounces	29.57	milliliters	mL
gal	gallons	3.785	liters	L
ft <sup>3</sup>	cubic feet	0.028	cubic meters	m <sup>3</sup>
yd <sup>3</sup>	cubic yards	0.765	cubic meters	m <sup>3</sup>
NOTE: volumes greater than 1000 L shall be shown in m <sup>3</sup>				
<b>MASS</b>				
oz	ounces	28.35	grams	g
lb	pounds	0.454	kilograms	kg
T	short tons (2000 lb)	0.907	megagrams (or "metric ton")	Mg (or "t")
<b>TEMPERATURE (exact degrees)</b>				
°F	Fahrenheit	5 (F-32)/9 or (F-32)/1.8	Celsius	°C
<b>ILLUMINATION</b>				
fc	foot-candles	10.76	lux	lx
fl	foot-Lamberts	3.426	candela/m <sup>2</sup>	cd/m <sup>2</sup>
<b>FORCE and PRESSURE or STRESS</b>				
lbf	poundforce	4.45	newtons	N
lbf/in <sup>2</sup>	poundforce per square inch	6.89	kilopascals	kPa
<b>APPROXIMATE CONVERSIONS FROM SI UNITS</b>				
Symbol	When You Know	Multiply By	To Find	Symbol
<b>LENGTH</b>				
mm	millimeters	0.039	inches	in
m	meters	3.28	feet	ft
m	meters	1.09	yards	yd
km	kilometers	0.621	miles	mi
<b>AREA</b>				
mm <sup>2</sup>	square millimeters	0.0016	square inches	in <sup>2</sup>
m <sup>2</sup>	square meters	10.764	square feet	ft <sup>2</sup>
m <sup>2</sup>	square meters	1.195	square yards	yd <sup>2</sup>
ha	hectares	2.47	acres	ac
km <sup>2</sup>	square kilometers	0.386	square miles	mi <sup>2</sup>
<b>VOLUME</b>				
mL	milliliters	0.034	fluid ounces	fl oz
L	liters	0.264	gallons	gal
m <sup>3</sup>	cubic meters	35.314	cubic feet	ft <sup>3</sup>
m <sup>3</sup>	cubic meters	1.307	cubic yards	yd <sup>3</sup>
<b>MASS</b>				
g	grams	0.035	ounces	oz
kg	kilograms	2.202	pounds	lb
Mg (or "t")	megagrams (or "metric ton")	1.103	short tons (2000 lb)	T
<b>TEMPERATURE (exact degrees)</b>				
°C	Celsius	1.8C+32	Fahrenheit	°F
<b>ILLUMINATION</b>				
lx	lux	0.0929	foot-candles	fc
cd/m <sup>2</sup>	candela/m <sup>2</sup>	0.2919	foot-Lamberts	fl
<b>FORCE and PRESSURE or STRESS</b>				
N	newtons	0.225	poundforce	lbf
kPa	kilopascals	0.145	poundforce per square inch	lbf/in <sup>2</sup>

\*SI is the symbol for the International System of Units. (Adapted from FHWA report template, Revised March 2003)



## **LIST OF ACRONYMS**

AI	Artificial Intelligence
CCTV	Closed-Circuit Television System
CNN	Convolutional Neural Network
DA	Data Augmentation
FHWA	Federal Highway Administration
GAN	Generative Adversarial Network
LSTM	Long Short-Term Memory
RNN	Recurrent Neural Network
RWIS	Road Weather Information System
UDOT	Utah Department of Transportation
YOLO	You Only Look Once

## **EXECUTIVE SUMMARY**

Traffic safety is significantly impacted by snow cover on road surfaces, contributing to 24 percent of annual weather-related vehicle crashes, according to the Federal Highway Administration. In Utah, the snow season can last up to seven months with over 25 winter storms annually, making real-time snow-cover data crucial for effective snow plow management by the Utah Department of Transportation (UDOT) and for public safety. Traditional methods for assessing road conditions rely on the Road Weather Information System (RWIS), which has limited coverage. The lack of information on snow cover conditions in non-RWIS locations complicates UDOT's ability to accurately know the roadway conditions in those locations.

This project utilizes image data from existing roadside Closed-Circuit Television System (CCTV) cameras to develop a deep learning-based AI model for automatic evaluation of snow-cover conditions. The methodology includes processing images to create labeled datasets, developing AI models based on the AlexNet architecture as the deep learning algorithm, and implementing these models to analyze real-time snow-cover conditions. Additionally, a weather interpolation method is developed to estimate real-time weather status in non-RWIS areas. The AI models are trained to classify snow-cover conditions into categories such as full snow-cover, partial snow-cover, and clear.

The developed AI models demonstrated high accuracy in identifying snow-cover conditions, achieving an overall accuracy exceeding 97 percent. Detailed confusion and performance matrices illustrate the models' ability in detecting various snow-cover states. This enables UDOT to monitor snow-cover on roads without additional costs. By leveraging existing CCTV networks, the project provides a cost-effective solution for large-scale, real-time road condition monitoring. The automated system processes and shares snow-cover information in an easily understandable format.

The project concludes that the developed AI models and weather interpolation method could significantly enhance UDOT's ability to monitor road conditions in non-RWIS areas. The automated system allows for more efficient snow plow planning and real-time road condition monitoring, improving safety and operational efficiency. It is recommended that UDOT

implements this AI-based approach to complement existing RWIS networks and provide real-time snow-cover information in non-RWIS locations.

This project offers a cost-effective, automated solution for monitoring snow-cover conditions on roads, closing information gaps in non-RWIS areas. The AI model and weather interpolation method have the potential to improve UDOT's snow plow management, enhance public safety, and provide real-time, easily understandable snow-cover information. The system's scalability and efficiency make it a valuable tool for statewide application, reducing weather-related vehicle crashes and improving road safety during winter seasons.

## **1.0 INTRODUCTION**

### **1.1 Problem Statement**

Traffic safety is negatively affected by snow cover on road surfaces during snowfalls. According to the Federal Highway Administration, 24 percent of annual weather-related vehicle crashes occur on snowy, slushy, or icy pavement, and 15 percent happen during snowfall or sleet, causing tremendous property losses, human injuries, and even deaths. In Utah, road safety is a serious concern in the snow season, which could last as long as ~7 months with >25 winter storms on average per year. During snowfalls, snow plowing is necessary to clear the snow on pavement surfaces to ensure roads are drivable. For UDOT, understanding real-time snow-cover conditions on roads is the premise to plan the optimal route of snow plows and clean up snow-cover in a timely manner. Meanwhile, providing snow-cover information of road surfaces is also useful to the public to further increase their safety awareness and avoid icy roads in driving.

To assess road surface conditions in snowfalls, the Road Weather Information System (RWIS) is commonly used. However, RWIS stations are not available to monitor snow-cover conditions in all sections of roads. In this case, the information collection of snow cover conditions in non-RWIS locations becomes difficult. This inevitably complicates UDOT's ability to accurately know the roadway conditions in those locations. Therefore, understanding snow plow performance and snow-cover conditions in not only RWIS areas, but also non-RWIS areas is significant for both UDOT maintenance crews and road users during the winter season. Hence, there is an urgent need to develop a comprehensive and efficient system that leverages AI and existing CCTV infrastructure to monitor snow-cover conditions in both RWIS and non-RWIS areas, ensuring timely and accurate information collection for improved snow plow management and enhanced road safety.

### **1.2 Research Objectives**

The primary objective of this project is to develop usable AI algorithms capable of automatically detecting snow-cover conditions on road surfaces using image data from existing roadside CCTV cameras. The project aims to integrate these AI models with a weather interpolation method to provide comprehensive and real-time evaluations of snow-cover in both

RWIS and non-RWIS locations, helping UDOT to understand real-time snow-cover conditions on roads as the premise to plan the optimal route of snow plows and clean up snow-cover in a timely manner.

### **1.3 Research Scope**

The project consists of five main research tasks (listed below), i.e., literature review, data collection and processing, developing AI algorithms for snow cover detection, as well as a weather interpolation method, and preparing the final project report. The primary source of data is the real-time and historical images provided by UDOT (from the RWIS and traffic management system). The five specific tasks are detailed below:

Task 1: Literature Review: review existing technologies and current practices in assessment of snow cover conditions on road surfaces and weather interpolation.

Task 2: Data Collection and Processing: image collection and labeling from RWIS stations and existing CCTV networks.

Task 3: Algorithm Development and Validation: develop and validate the snow cover condition evaluation model based on computer vision and deep learning techniques.

Task 4: Weather Information Interpolation: interpolate weather data for non-RWIS locations.

Task 5: Project report preparation: prepare the final project report.

### **1.4 Outline of Report**

The remaining report is structured as follows: Section 2 reviews the pros and cons of different methods as current practices in snow-cover condition assessment and weather interpolation. Section 3 introduces the methods used in this project and accuracy metrics to measure the algorithm development performance. The results and performance of the developed AI models for snow-cover condition identification and weather information interpolation are in Section 4. Section 5 summarizes the key findings and recommendations for future work. Finally, Section 6 contains future steps and required resources to implement the developed AI model in practice.

## **2.0 LITERATURE REVIEW**

### **2.1 Data Collection and Processing**

The images used in this project are primarily real-time and historical images from the RWIS system. Due to this year's mild winter, as well as issues such as low resolution and logo obstructions, some techniques, including data augmentation, summer-to-winter image translation using Generative Adversarial Networks (GANs), and super resolution, are required to process the images before training the AI models to ensure the decent model performance in application.

#### **2.1.1 Data Augmentation**

Data augmentation is a crucial technique in machine learning that involves generating new training samples by applying various transformations to the existing dataset. This process helps to increase the diversity of the data without collecting additional images, thereby enhancing the robustness and performance of the AI models. The first significant application of data augmentation in computer vision was on the ImageNet dataset. Alex Krizhevsky et al. demonstrated the importance of data augmentation in computer vision, showcasing its effectiveness in improving model performance (Krizhevsky et al., 2017). Data augmentation includes rotation, flipping, scaling, noise addition, padding, etc., as shown in Figure 1. By applying these data augmentation techniques, the dataset is significantly expanded, providing a more comprehensive set of training samples. This helps to improve the generalization capabilities of the AI model, making it more effective in real-world scenarios where snow-cover conditions can vary widely.



**Figure 1 Data Augmentation Example**

### 2.1.2 Summer-to-Winter Image Translation Using GANs

GANs are a class of machine learning frameworks designed by Ian Goodfellow and his colleagues in 2014 (Goodfellow et al., 2014). GANs consist of two neural networks: a generator and a discriminator. These two networks are trained simultaneously through a process of adversarial learning. The generator and discriminator are in a constant adversarial game where the generator tries to produce increasingly realistic data, and the discriminator aims to get better at distinguishing real data from fake data. This process continues until the generator produces data that is indistinguishable from real data, fooling the discriminator.

One popular application of GANs is image translation, where GANs are used to transform images from one domain to another, such as converting summer scenes to winter scenes, which is one of the potential methods to address the issue of insufficient snow-cover image data (Mingjian Wu et al., 2023), (Gong et al., 2024). Figure 2 shows examples of the results of GANs training.

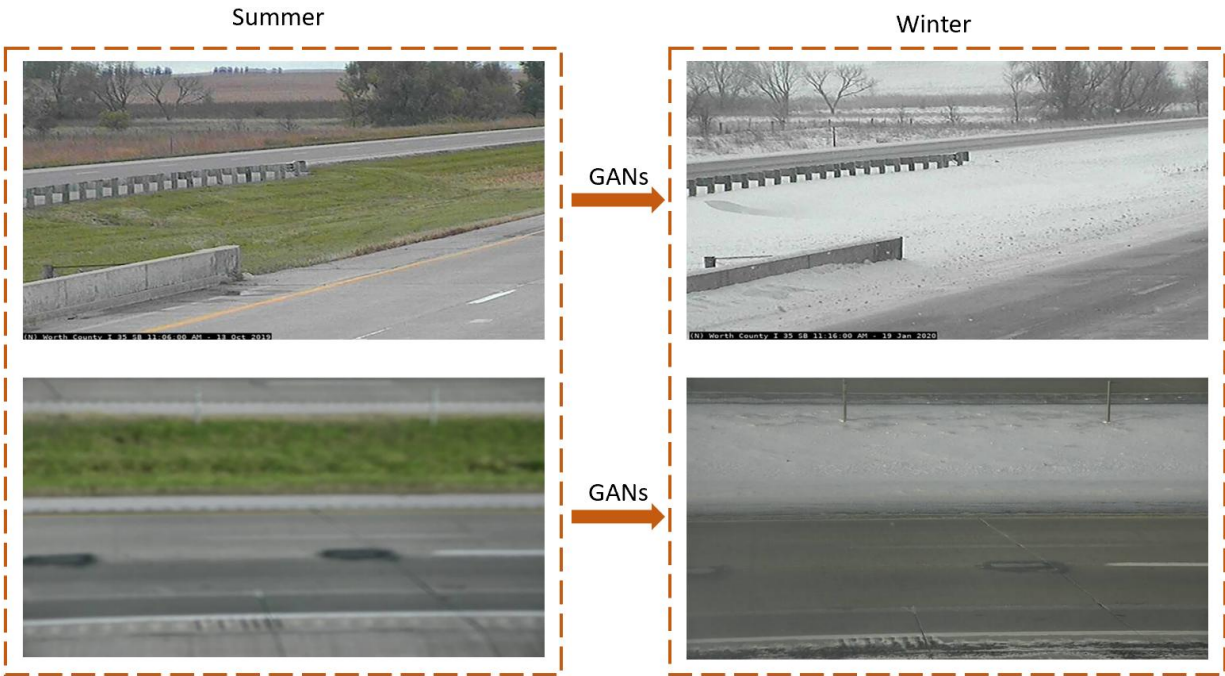


**Figure 2 Examples of GANs results (Mingjian Wu et al., 2023)**

However, GANs have several drawbacks, including training instability, mode collapse, and sensitivity to hyperparameters, which make them challenging to optimize (Oriol & Miot, 2021). They also require significant computational resources and large datasets to produce high-quality outputs. Additionally, the lack of universally accepted evaluation metrics complicates the assessment of GAN-generated images, and ensuring convergence during training can be difficult. Despite their potential, these limitations can hinder the effective deployment of GANs in various applications.

### 2.1.3 Super Resolution

Super resolution is a technique in image processing that aims to enhance the resolution of an image, increasing its pixel density and improving its visual quality (Lepcha et al., 2023). This process can convert a low-resolution image into a high-resolution version, revealing more details and producing clearer images. Figure 3 shows an example of super resolution. Super-Resolution Generative Adversarial Network (SRGAN) is a type of GAN designed specifically for image super-resolution, which is the process of enhancing the resolution of an image (Ledig et al., 2016). SRGAN can significantly improve the quality and detail of low-resolution images compared to



other super-resolution methods, making it valuable for applications requiring high-resolution outputs. The structure of SRGAN is shown in Figure 4.

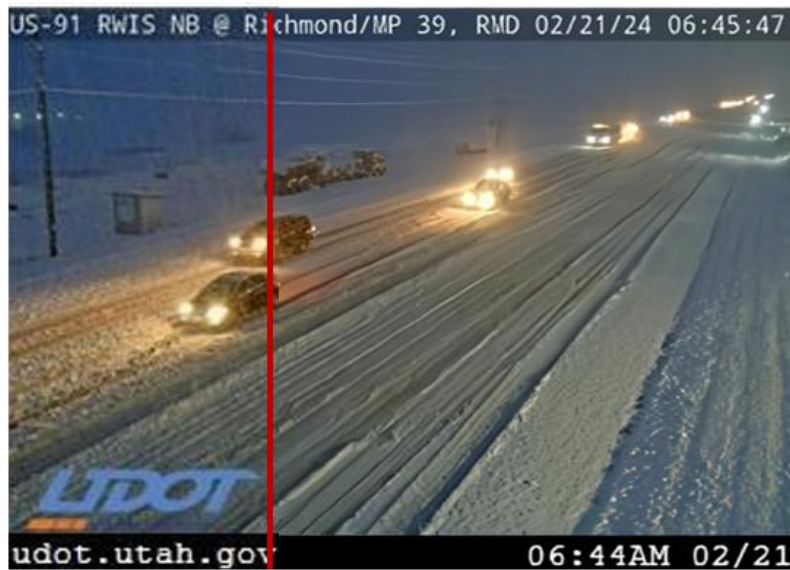


Figure 3 Example of super resolution

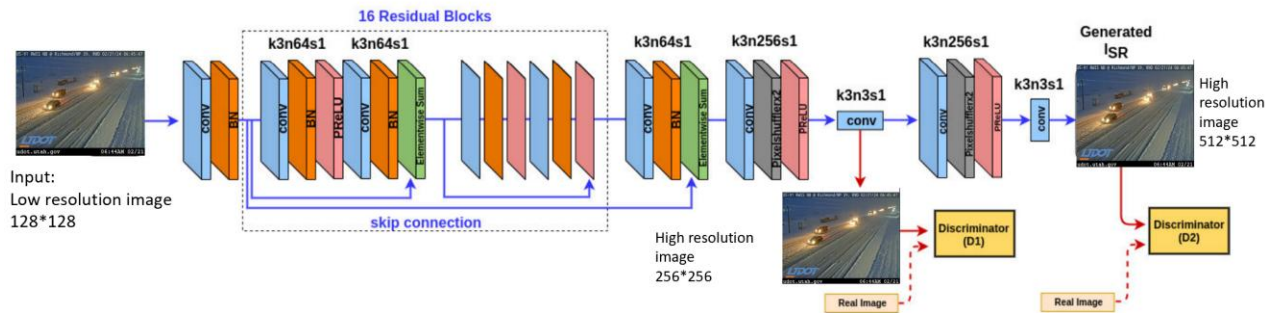


Figure 4 The structure of SRGAN

### 2.1.4 Brief Summary

Data augmentation (DA), GANs, and super resolution are powerful techniques employed to tackle different challenges in image processing and machine learning. Data augmentation increases the diversity of the training dataset, thereby mitigating the problem of insufficient data. GANs are used to generate realistic synthetic data and enhance existing datasets, addressing the issue of data scarcity and diversity. Super resolution improves the quality of low-resolution images,

ensuring that finer details are captured for more accurate analysis. By effectively applying these techniques, it is possible to address the issues of insufficient data and low-quality images, ultimately enhancing the accuracy and robustness of CNNs.

## **2.2 Road Surface Condition Recognition AI Models**

AI models (e.g., computer vision and deep learning) perform well in automatic object detection and image classification. Currently, these AI models have been applied in the assessment of weather and road surface conditions.

### 2.2.1 Artificial Intelligence Models

Computer vision is an interdisciplinary research area to understand the underlying physical world by extracting and analyzing valuable information from images or videos (Huang et al., 2021). Image analysis and object detection by computer are similar to visual inspection by human inspectors due to the information captured by images or videos which is analogous to that obtained by humans (Spencer et al., 2019). From low-level to high-level processing, computer vision includes image acquisition, segmentation, feature extraction, object recognition, and structure analysis (Koch et al., 2015).

Deep learning has a strong capability to interpret images, sounds, and text by mimicking the mechanisms of the human brain in interpretation. The frameworks of deep learning consist of multiple layers of neuron nodes, and the training dataset is used to solve the weights of the neural network and form the AI model finally (Lu, 2019). There are large numbers of deep learning frameworks available, such as You Only Look Once (YOLO) (Redmon et al., 2016), Convolutional Neural Networks (CNN), and Region-CNN (RCNN) (Krizhevsky et al., 2017). Compared with other deep learning methods that propose regions of interest first before convolution operation, YOLO performs detection and classification simultaneously (Redmon et al., 2016). This makes YOLO run faster than other algorithms (e.g., Faster RCNN) and achieve higher mean average precision (Redmon et al., 2016). Consequently, YOLO is proven to be an object detection model with high accuracy and speed among deep learning models.

In recent years, due to the high accuracy and fast inference speed of deep learning, it has fueled significant strides in various computer vision problems, including object detection and image segmentation (Voulodimos et al., 2018). Compared to traditional computer vision algorithms, deep learning has many advantages. Traditional computer vision algorithms use certain programming paradigms to extract features, which needs a lot of trial and error to select the appropriate ones (O'Mahony et al., 2020). On the other hand, deep learning directly uses a training framework with a set of inputs and known outputs, which alleviates the tedious process of feature extraction and signal processing (O'Mahony et al., 2020). Second, deep learning can achieve better performance compared to other traditional computer vision methods, especially in big data analysis, e.g., video data processing and analysis (Huang et al., 2021).

### 2.2.2 Applications of AI Models in Road Surface Condition Detection

The use of in-vehicle camera systems has been extensively studied for detecting weather and road surface conditions. For instance, Qian et al. developed a system using static images from a dashboard camera to classify road weather conditions, achieving 80 percent accuracy for clear and snow/ice-covered images and 68 percent accuracy for clear/dry, wet, and snow/ice-covered images (Qian et al., 2016). A recent study leveraged the SHRP2 Naturalistic Driving Study (NDS) data to create a fog detection system by applying various machine learning algorithms, including Recurrent Neural Network (RNN), Long Short-Term Memory (LSTM), and Convolutional Neural Network (CNN). This system was able to detect trajectory-level weather with an overall accuracy exceeding 97 percent (Khan & Ahmed, 2021). Additionally, Kawai et al. proposed a method to differentiate road surface conditions at night using images extracted from an inexpensive car-mounted video camera, achieving accuracies of 96, 89, and 96 percent for distinguishing dry, wet, and snowy road conditions, respectively (Kawai et al., 2014). Madiha et al. pointed out that road weather detection should consider multi-class classification, such as snowy and icy conditions. They proposed a vision transformer with attention mechanisms to create a multi-label weather dataset for roads, addressing the issue of multiple weather conditions existing in a single frame (Samo et al., 2023). Zhao et al. proposed a CNN-RNN based multi-label classification approach to address this issue. The CNN is extended with a channel-wise attention model to extract the most correlated visual features. The RNN further processes these features and uncovers the

dependencies among weather classes. Ultimately, their model achieved an accuracy of 91.35 percent (Zhao et al., 2018).

In addition to in-vehicle camera systems, the use of fixed cameras to detect weather and surface conditions has also been explored in the literature. This approach utilizes weather data and camera images from the Road Weather Information System (RWIS) and Closed-Circuit Television system (CCTV). Carrillo et al. collected 70,000 weather measurements from RWIS and compared the performance of several deep learning models, including DenseNet, NASNet, and MobileNet, and showed an accuracy of around 91 percent (Carrillo et al., n.d.). Sirirattapol et al. utilized CCTV images to develop a road environment extraction framework that considers various conditions (e.g., raining and non-raining, dry and wet roads), resulting in 93 percent accuracy (Sirirattapol et al., 2019). Khan et al. utilized images from Department of Transportation (DOT) webcams, applying AlexNet, GoogLeNet, and ResNet18 with appropriate modifications through transfer learning to achieve classification tasks. They achieved an accuracy rate of up to 97.3 percent (Khan & Ahmed, 2022).

### 2.2.3 Weather Interpolation

Weather Interpolation provides climatological and meteorological data products covering the whole country as maps or gridded datasets. Alain et al. proposes a new method to efficiently combine weather radar data with data from two non-collocated heated rain gauge networks using a regression co-kriging approach, demonstrating improved performance over traditional methods like inverse distance weighting, especially in complex Alpine topographies (Foehn et al., 2018). Adam M. Wilson's study employs a climate-aided Bayesian kriging approach to interpolate 20 years of daily meteorological observations, producing high-resolution climate metric surfaces with associated uncertainties for the Cape Floristic Region of South Africa. This work enhances predictive modeling in ecology and biogeography (Wilson & Silander, 2014). Similarly, Jordan P. Brook et al. introduced a variational gridding method for weather radar data that outperforms existing methods in data resolution, noise filtering, and spatial continuity, offering significant potential improvements for applications in meteorological research and forecasting (Brook et al., 2022).

#### 2.2.4 Brief Summary

Overall, this section explores the application of artificial intelligence (AI) models, particularly in computer vision, for detecting weather and road surface conditions. It discusses the advantages of deep learning over traditional computer vision methods, highlighting various studies that utilize AI models like CNN, RNN, LSTM, and YOLO for accurate weather and road condition detection. The research includes the use of in-vehicle and fixed cameras, with notable success in different weather scenarios. Additionally, this section covers weather interpolation methods, emphasizing innovative approaches like regression co-kriging and Bayesian kriging, which enhance predictive modeling by efficiently combining radar data with rain gauge networks.

### 3.0 METHODOLOGY

#### 3.1 Research Process Overview

The overall workflow of AI model development for this study is shown in Figure 5. Road condition images were collected from CCTV cameras and RWIS. These collected images were then converted into three categories and labeled for AI model training and testing. Specifically, these labeled images underwent preprocessing methods such as super-resolution and logo inpainting to train the artificial intelligence model. Model tests were then performed using the test images to identify remaining issues in road condition detection. Then, weather station information including coordinates of Weather Stations, rainfall data, and snowfall data was collected to facilitate weather interpolation and predict real-time weather information in non-RWIS and non-CCTV areas.

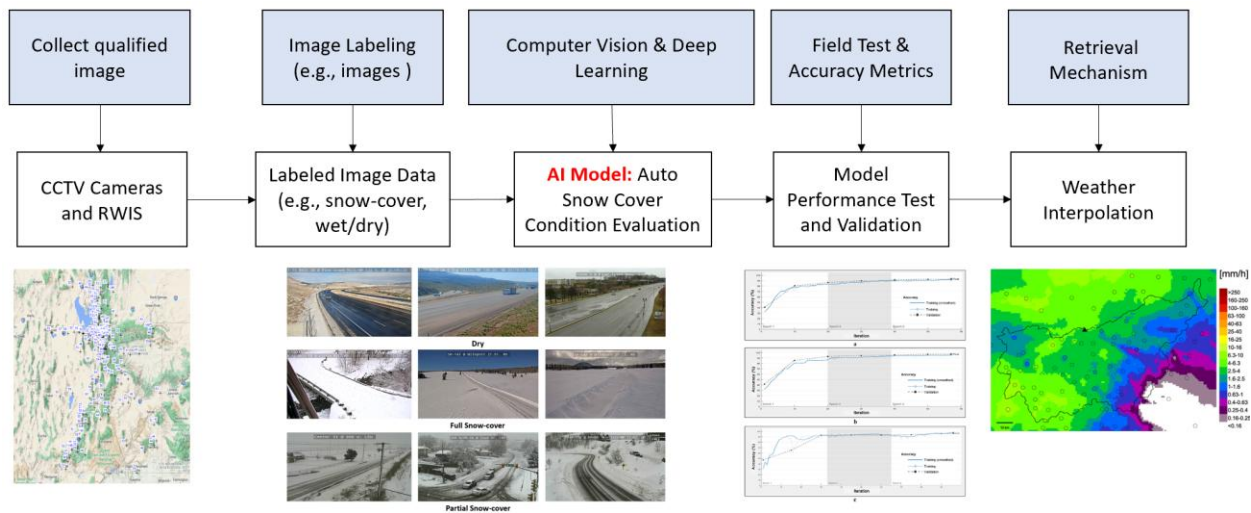


**Figure 5 Flowchart of Model Development and Improvement**

#### 3.2 Data Collection and Processing

UDOT provided a Filezilla account to share the historical road images from CCTV cameras in Utah. The photos will be updated periodically. The training and test datasets will be selected based on the criteria that the webcams at each location captured images of at least three views of

the roadways, including westbound, eastbound, and the road surface. The Filezilla Interface is shown in Figure 6.

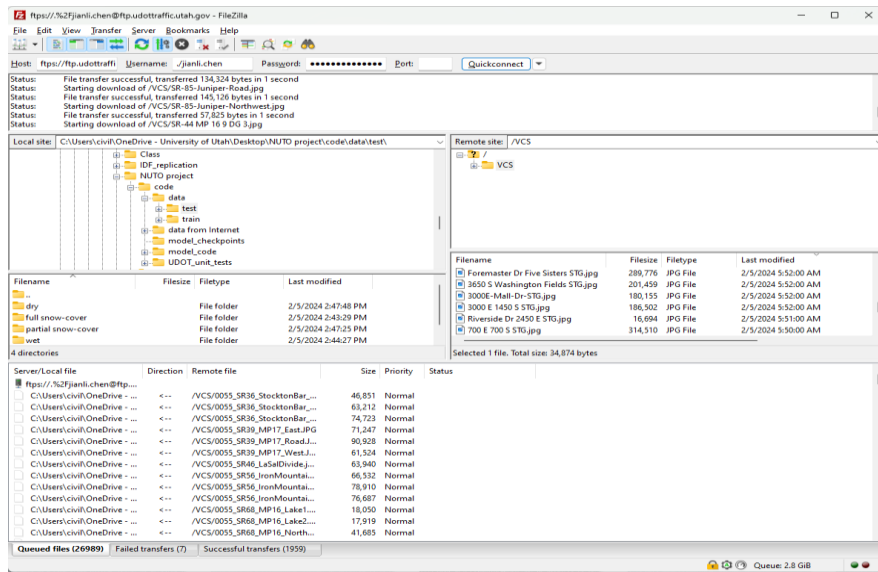


**Figure 6 The Filezilla Interface**

Additionally, UDOT provided historical images from over 100 RWIS stations as shown in Figure 7. These images typically have low resolution, noticeable logos, and small sizes. To address these issues, techniques such as super resolution and logo inpainting are employed, as shown in Figure 8. Super resolution improves image clarity by using advanced algorithms and deep learning models to enhance low-resolution images, effectively increasing their pixel count and overall size. This results in clearer, more detailed images suitable for detailed analysis. Logo inpainting, on the other hand, removes unwanted logos or watermarks by detecting and eliminating them, then filling in the gaps with visually consistent content. This process enhances image quality by ensuring that critical features like road surface conditions are unobstructed and clearly visible. Together, these techniques transform the historical images into high-quality, usable data.

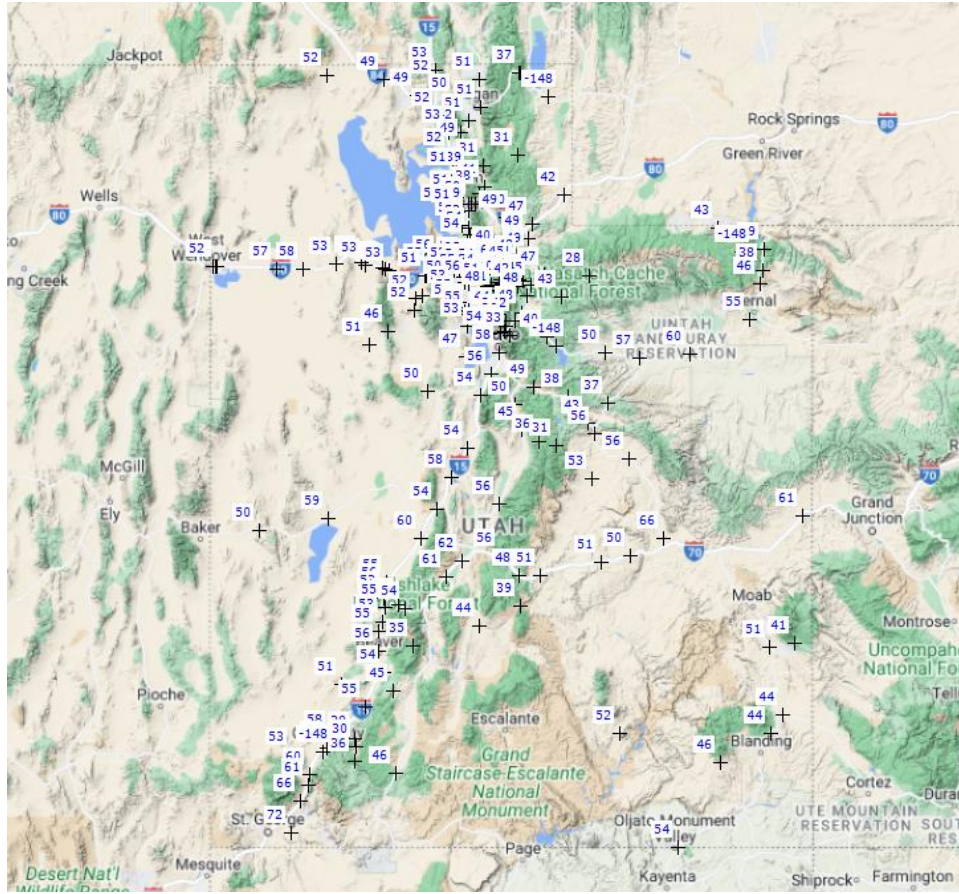
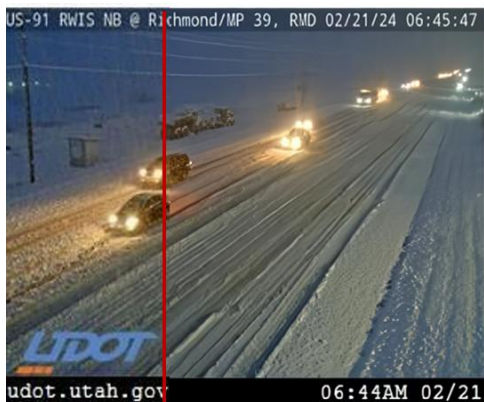


**Figure 7 100+ RWIS sites**



(a)



(b)

**Figure 8 Processing techniques (a) super resolution (b) logo inpainting**



### 3.3 Data Annotations

After collecting and processing the data, we will label it according to the following criteria:

- (a) Clear: The road surface is clean, free of precipitation, and has no or little snowfall. This includes both wet and dry conditions.
- (b) Partial Snow-Cover: The road surface is partially covered with snow, with sections of the road still visible.
- (c) Full Snow-Cover: Most of the road surface is covered with snow.

Each data point will be evaluated and categorized based on these definitions to ensure consistent and accurate labeling, which is crucial for subsequent model training and validation.

**Table 1 Summary statistics of the image datasets**

Category	Total	Training dataset	Test dataset
Clear	4059	2783	1276
Partial snow-cover	603	433	170
Full snow-cover	239	160	79



Clear

Partial Snow-Cover

Full Snow-Cover

**Figure 9 Sample image of road conditions**

## **3.4 Training of AlexNet as the Deep Learning Algorithm for Automated Road Condition Evaluation**

Following the data collection, processing, and annotation stages described above, the next step involves training of the AI model, specifically using the AlexNet architecture. The training process is designed to fine-tune the AI model to accurately classify and assess road conditions.

### 3.4.1 Preparation of Training and Test Datasets

The annotated datasets from Section 3.3 are divided into training and test sets. The training set is used to teach the model, while the test set is reserved for evaluating its performance. The datasets include images categorized as Clear, Partial Snow-Cover, and Full Snow-Cover.

### 3.4.2 Model Architecture: AlexNet

AlexNet, a convolutional neural network (CNN) architecture, is employed for this task due to its proven efficacy in image classification and feature extraction. AlexNet consists of multiple layers, including convolutional layers, pooling layers, and fully connected layers, which work together to learn the intricate patterns in the input images.

- (a) Convolutional Layers: These layers apply convolutional filters to the input images, detecting essential features such as edges, textures, and shapes.
- (b) Pooling Layers: These layers reduce the spatial dimensions of the feature maps, which helps in reducing computational complexity and preventing overfitting.
- (c) Fully Connected Layers: These layers act as a classifier based on the features extracted by the convolutional layers, assigning probabilities to each class (Clear, Partial Snow-Cover, Full Snow-Cover).

### 3.4.3 Training Process

The training of AlexNet involves the following main steps:

- (a) **Data Augmentation:** To enhance the robustness of the model, data augmentation techniques are applied. This includes random rotations, shifts, and flips of the input images, ensuring that the model can generalize well to various real-world scenarios.
- (b) **Loss Function:** The cross-entropy loss function is used to measure the discrepancy between the predicted labels and the true labels. This function is particularly effective for classification tasks.
- (c) **Optimizer:** The Adam optimizer, known for its efficiency and adaptive learning rate, is used to update the model weights during training. This helps in achieving faster convergence and better performance.
- (d) **Training Loop:** The model is trained over several epochs, where each epoch represents a full pass through the training dataset. During each epoch, the model's weights are adjusted to minimize the loss function.
- (e) **Validation:** The performance of the model is periodically validated using the test dataset. Key metrics such as accuracy, precision, recall, and F1-score are tracked to evaluate how well the model is learning and to prevent overfitting.
- (f) **Hyperparameter Tuning:** Hyperparameters such as learning rate, batch size, and number of epochs are fine-tuned to achieve the best possible performance.

### 3.5 Accuracy Metrics

The metrics of AlexNet training are defined as follows:

$$Accuracy = \frac{TP + TN}{TP + TN + FP + FN}$$

$$Precision = \frac{TP}{TP + FP}$$

$$Recall = \frac{TP}{TP + FN}$$

$$F1\ Score = \frac{2 * Precision * Recall}{Precision + Recall}$$

TP describes the true positive, i.e., a positive object is captured by a prediction box, while a false positive (FP) dictates that a prediction box is made but captures a wrong object. Likewise, false negative (FN) means that a positive object is not detected with any prediction box. True negative (TN) represents cases where the model correctly identifies a negative instance. The precision reflects the reliability in classifying objects as positive, while the recall measures the model's ability to detect positive objects (i.e., TP). To avoid outperforming in one of the two metrics (i.e., precision and recall) but underperforming in the other, F1-score is introduced to balance recall and precision by weighting them equally (Arya et al., 2020). In the reported metrics, since our objective is to identify the interested objects, these objects will be marked as true positive as long as they are captured by the developed AI algorithms in the video detection process.

### **3.6 Weather Interpolation**

The weather interpolation method was developed in this study to estimate real-time weather status in non-RWIS areas. Section 3.6 covers the methodology for weather interpolation, starting with the data collection process (3.6.1) and followed by the application of Radial Basis Function (RBF) interpolation techniques (3.6.2) to accurately estimate weather conditions across different locations.

#### **3.6.1 Data Collection**

The dataset for the weather interpolation has been collected from various meteorological stations in the Salt Lake City region and Northern Utah, ensuring a comprehensive representation of different weather parameters. The data was obtained from Synoptic Data, a reliable source for high-quality meteorological information. The data includes several crucial weather variables measured at numerous stations and is shown in Table 2. The collected data is visualized in maps to provide a clear spatial distribution of the meteorological stations and the corresponding weather parameters (Figure 10). In the Salt Lake City area, there is a dense network of stations within the defined region. The red and orange markers represent the stations recording temperature, humidity, wind speed, and precipitation. The boundary of this area is marked to highlight the coverage extent of the data

collection effort. However, there are just four stations that collect snow data, which is limited for interpolation. Thus, we enlarge the collection area for snow data from the Salt Lake City area to the Northern Utah region. In Northern Utah, the figure illustrates a broader region for snow data with stations marked in green.

The data was acquired from Synoptic Data by calling API. This platform provides real-time and historical weather data from a network of meteorological stations. The steps involved in the data collection process are as follows: 1) identifying and selecting meteorological stations within the target regions that provide reliable and continuous weather data; 2) calling API for downloading the relevant weather parameters for the specified dates, ensuring data completeness and accuracy; 3) processing the raw data to remove any anomalies or missing values, ensuring that the dataset is robust and ready for interpolation; and 4) mapping the stations and their recorded data to visualize the spatial distribution and identify any gaps in coverage. This comprehensive dataset serves as the foundation for the RBF interpolation process, enabling accurate and detailed weather interpolations across the specified regions. The meticulous data collection process ensures that the interpolated results are based on high-quality and representative weather data, which is crucial for reliable weather analysis and forecasting.

**Table 2 Weather variables and regions of stations**

Variables	Number of stations	Time	Region
Air temperature	167	07.28.2024	Salt Lake City
Relative humidity	143	07.28.2024	Salt Lake City
Wind speed	147	07.28.2024	Salt Lake City
Precipitation (24 hr)	44	07.28.2024	Salt Lake City
Snow (24 hr)	44	01.04.2024	Northern Utah

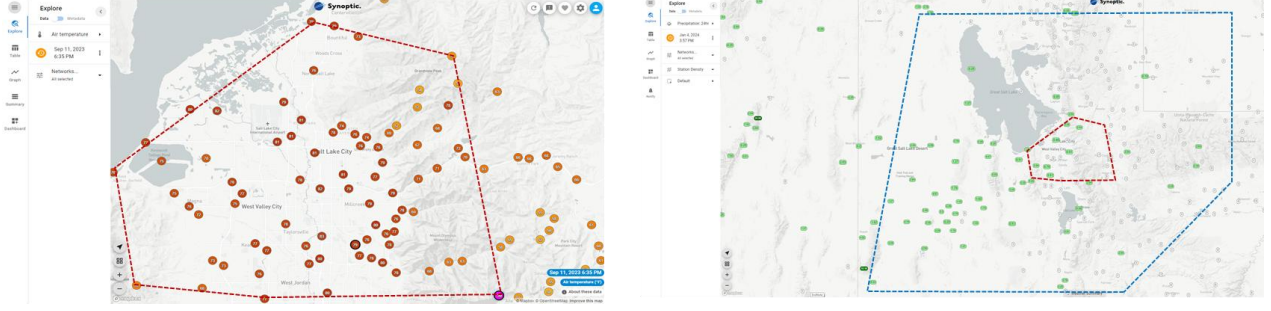


**Figure 10 Regions and stations for weather data collection**

### 3.6.2 Radial Basis Function (RBF) Interpolation

Radial Basis Function (RBF) interpolation is a powerful method for spatial interpolation of scattered data, such as weather data, which is often collected at irregularly spaced meteorological stations. This methodology details the steps and principles behind using RBF interpolation, specifically focusing on two commonly used basis functions: multiquadric and thin plate spline. RBF interpolation is a technique that reconstructs a smooth function from discrete data points by using radial basis functions centered at the data points. The interpolated value at any given location is a weighted sum of the basic functions. Mathematically, the interpolated value  $f(x)$  at a point  $x$  can be expressed as:

$$f(x) = \sum_{t=1}^N w_t \phi(\|x - x_t\|) + P(x), \quad (1)$$

where  $N$  is the number of data points;  $w_t$  are the weights;  $x_t$  are the locations of the data points;  $\phi(r)$  is the radial basis function;  $\|x - x_t\|$  is the Euclidean distance between  $x$  and  $x_t$ ;  $P(x)$  is a low-order polynomial (optional, for ensuring polynomial reproduction). Two popular choices for the radial basis function  $\phi(r)$  are Multiquadric (MQ) and Thin Plate Spline (TPS). The multiquadric basis function is defined as:

$$\phi(r) = \sqrt{r^2 + c^2}, \quad (2)$$

where  $c$  is a positive constant. The parameter  $c$  controls the shape of the basis function, with larger values leading to smoother interpolations. The multiquadric function tends to provide

good results for a wide range of interpolation problems due to its flexibility and smoothness. The thin plate spline basis function is defined as:

$$\phi(r) = r^2 \ln(r), \quad (3)$$

This function is derived from the physical analogy of bending a thin metal plate and is particularly effective for smooth, continuous surfaces. TPS is known for its robustness in handling irregularly spaced data and producing smooth interpolated surfaces. RBF interpolation, with multiquadric and thin plate spline basis functions, offers a robust and flexible approach to weather data interpolation. By carefully selecting parameters, preprocessing data, and implementing efficient computational techniques, accurate and smooth interpolations can be achieved, providing valuable insights for weather analysis and forecasting.

## 4.0 AI MODEL DEVELOPMENT

### 4.1 Performance of the Developed AI Model

Our total dataset consists of 4901 images, with 3376 images for training and 1525 images for testing, used to evaluate the trained AI model for road condition detection. The training phase includes a total of 25 epochs, achieving an overall training accuracy of 99.38 percent and an overall testing accuracy of 97.44 percent (Figure 11). Figure 12 presents the confusion matrix for the different categories. Table 3 summarizes the classification performance metrics, including precision, recall, and F1 Scores.

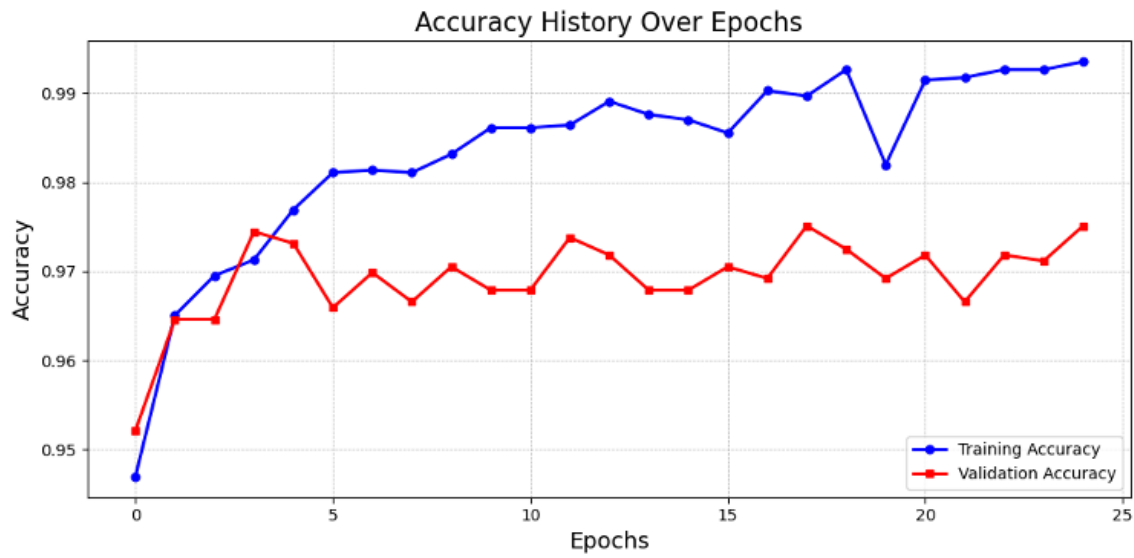


**Figure 11 Training and validation accuracy history over epochs**



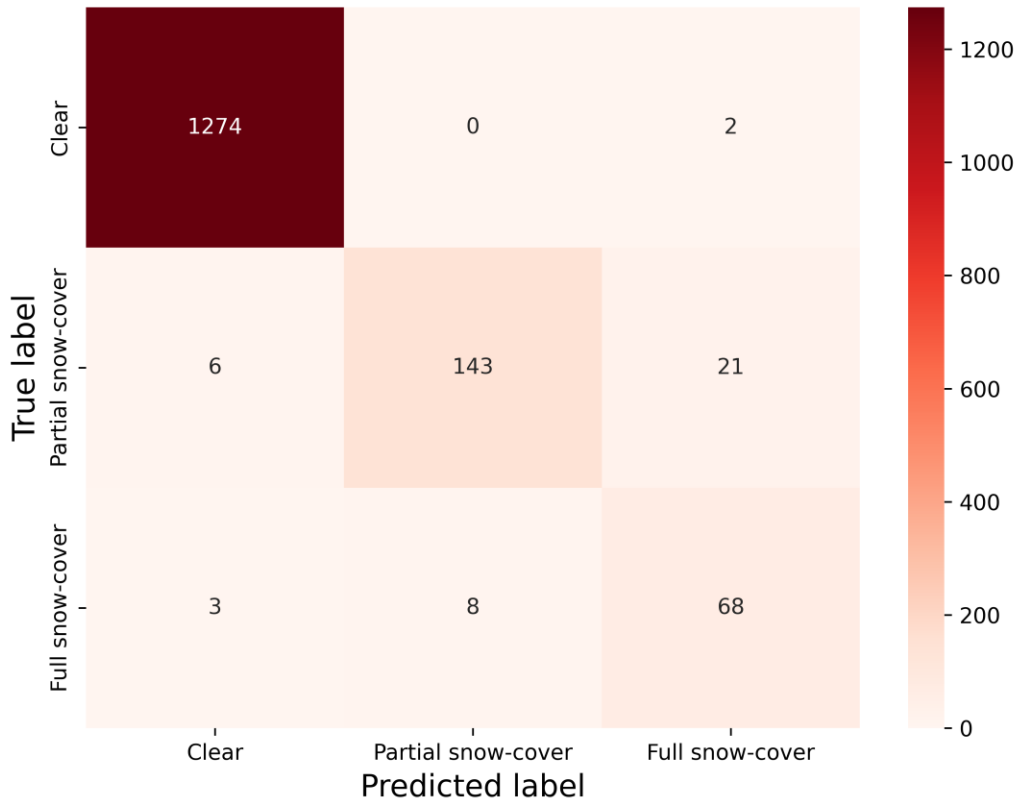


**Figure 12 Confusion matrix for the test dataset**

**Table 3 Classification performance metrics for the test dataset**

Class	Precision	Recall	F1 Score
Clear	0.993	0.998	0.891
Partial snow-cover	0.947	0.841	0.800
Full snow-cover	0.747	0.861	0.996

The model's accuracy varies across different categories (clear, partial snow-cover, and full snow-cover) in classification. For the clear category, we collected 4059 images, with 2783 used for training and 1276 for testing. The accuracy for the clear category is 99 percent (Successfully

classified examples as shown in Figure 13). In the misclassified images, we found that all errors involved misclassifying the clear category as the full snow-cover category. By comparing correctly and incorrectly classified images, we observed that some clear category images contain strip-like snow patches on the roadside. This led the model to erroneously classify the roadside snow patches as full snow-cover on the road (Figure 14).



**Figure 13 Successfully classified clear category images**



**Figure 14 Misclassified clear category as partial snow-cover category**

For the partial snow-cover category, we collected 603 images, with 433 used for training and 170 for testing. The accuracy for the clear category is 84 percent (Successfully classified

examples as shown in Figure 15). In the misclassified images, we found that the partial snow-cover category may be misclassified as full snow-cover and clear categories. Specifically, 22.22 percent of the partial snow-cover images were misclassified as clear, and 77.78 percent were misclassified as full snow-cover. By comparing correctly and incorrectly classified images, we observed the following patterns:

1. **Partial snow-cover misclassified as clear:** These images typically contain clear tire tracks where the snow has been compressed by vehicles. Although there is significant snow accumulation in the middle and on the sides of the road, the visible tracks lead the model to incorrectly classify these images as clear (Figure 16).
2. **Partial snow-cover misclassified as full snow-cover:** These cases usually involve images with extensive snow coverage in the environment, leading the model to mistakenly identify them as full snow-cover (Figure 17).



**Figure 15 Successfully classified partial snow-cover category images**



**Figure 16 Misclassified partial snow-cover category as clear category**



**Figure 17 Misclassified partial snow-cover category as full snow-cover category**

For the full snow-cover category, we collected 239 images, with 160 used for training and 79 for testing. The accuracy for the clear category is 86 percent (Successfully classified examples as shown in Figure 18). In the misclassified images, we found that the full snow-cover category may be misclassified as partial snow-cover and clear categories. Specifically, 27.27 percent of the full snow-cover images were misclassified as partial snow-cover, and 72.73 percent were misclassified as clear. By comparing correctly and incorrectly classified images, we observed the following patterns:

1. **Full snow-cover misclassified as clear:** These images often contain a significant amount of noise elements, such as mountains and sky, which result in the snow-covered road occupying a smaller area of the image or making the snow-covered road

unrecognizable. Consequently, these images were incorrectly classified as clear (Figure 19).

2. **Full snow-cover misclassified as partial snow-cover:** This misclassification typically occurs due to the presence of vehicle tracks or shadows, causing slight markings on the snow-covered road, leading to an incorrect classification as partial snow-cover (Figure 20).



**Figure 18 Successfully classified full snow-cover category images**



**Figure 19 Misclassified full snow-cover category as clear category**

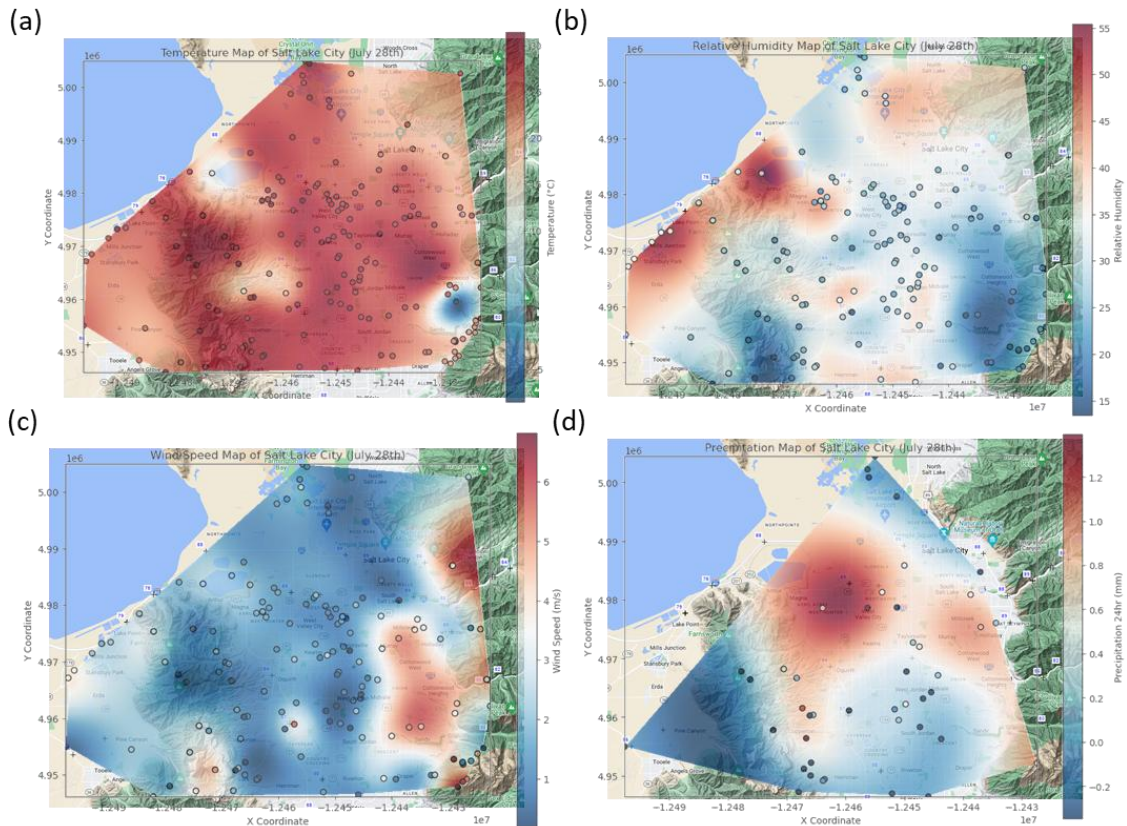


**Figure 20 Misclassified full snow-cover category as partial snow-cover category**

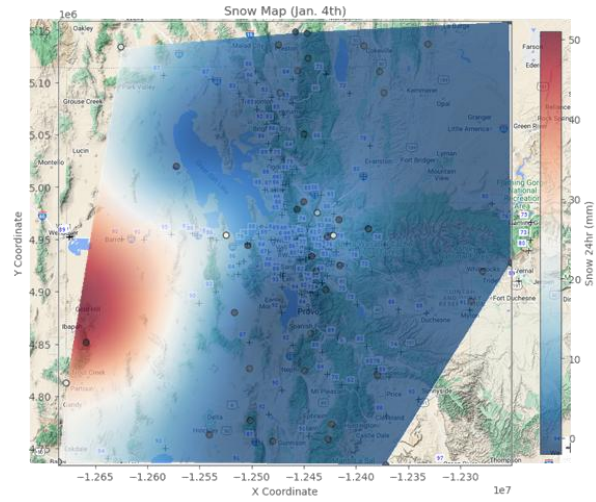
## 4.2 Weather Interpolation

Figure 21 presents the spatial interpolation results for various weather parameters in the Salt Lake City region and Northern Utah, using the Radial Basis Function (RBF) interpolation method. These maps provide a detailed view of the spatial distribution of air temperature, relative humidity, wind speed, precipitation, and snow accumulation, offering valuable insights into regional weather patterns. Figure 21.a depicts the interpolated air temperature across Salt Lake City on July 28, 2024. The color gradient ranges from blue, indicating lower temperatures, to red, representing higher temperatures, with data points marked by circles. It reveals significant temperature gradients, with the northwestern part of the region exhibiting higher temperatures, while cooler areas are observed toward the southeast. In Figure 21.b, the spatial distribution of relative humidity is illustrated, highlighting considerable variations in humidity levels, with drier conditions prevalent in the western parts and more humid conditions toward the eastern areas. Figure 21.c shows the spatial variation of wind speeds, revealing areas of higher wind speeds predominantly in the eastern part of the region, while calmer conditions are noted toward the west. Figure 21.d indicates the amount of rainfall over a 24-hour period. The map reveals a distinct spatial pattern, with higher precipitation observed in the northeastern areas and lower precipitation toward the southwest. Figure 22 presents the interpolated snow accumulation for Northern Utah on January 4, 2024. The color gradient ranges from blue, indicating less snow, to red, representing more snow, with data points marked by circles. This map shows significant snow accumulation in the western part of the region, particularly around higher elevations, while the eastern and central areas exhibit less snow.

The interpolated maps generated using the RBF interpolation method provide valuable insights into the spatial distribution of various weather parameters. The distinct patterns observed in temperature, humidity, wind speed, and precipitation maps for Salt Lake City, along with the snow accumulation map for Northern Utah, highlight the effectiveness of RBF interpolation in capturing spatial variability. These maps serve as essential tools for meteorologists and researchers in understanding regional weather patterns, aiding in weather prediction and planning.



**Figure 21 Weather interpolation in Salt Lake City. (a) Temperature (b) Relative humidity (c) Wind speed (d) Precipitation accumulation within 24 hours**



**Figure 22 Interpolation of snow accumulation within 24 hours in Northern Utah**



## **5.0 CONCLUSIONS**

### **5.1 Summary**

In this research, we utilized image data from existing roadside CCTV cameras to develop a deep learning-based AI model for the automatic evaluation of snow cover conditions of the roadway. The methodology includes processing images to create labeled datasets, developing AI models based on the AlexNet architecture, and implementing these models to analyze real-time snow-cover conditions. Additionally, a weather interpolation method was developed to estimate real-time weather status in non-RWIS areas.

### **5.2 Findings**

The developed AI model was trained to classify snow-cover conditions of the roadway into categories including full snow-cover, partial snow-cover, and clear. The model demonstrated high accuracy in identifying snow-cover conditions, achieving over 97 percent accuracy in detecting various snow-cover states. This enables UDOT to monitor snow-cover on roads without additional costs. By leveraging existing CCTV networks, the project provides a cost-effective solution for large-scale, real-time road condition monitoring.

In conclusion, this project offers a scalable, efficient, and cost-effective solution for monitoring snow-cover conditions on roads, ultimately reducing weather-related vehicle crashes and improving road safety during winter seasons. The developed AI models and weather interpolation method significantly enhance UDOT's ability to monitor road conditions in non-RWIS areas. The automated system allows for more efficient snow plow planning and real-time road condition monitoring, improving safety and operational efficiency.

### **5.3 Limitations and Future Work**

The AI model in this study faces issues of data imbalance and specific misclassification patterns in road condition detection. In the training and testing datasets, there are significantly more clear category images than partially and fully snow-covered category images, leading to

inferior performance of developed AI models to assess situations on these two categories. Additionally, images of clear roads with roadside snow are often misclassified as fully snow-covered, while partially snow-covered images with clear tire tracks are sometimes misclassified as clear. These misclassifications indicate that the model struggles with subtle variations within categories. Environmental elements such as mountains and the sky can occasionally cause fully snow-covered images to be misclassified. Therefore, future work should focus on data augmentation, improving feature extraction, noise reduction, extended testing, integration with real-time data, and interdisciplinary collaboration to enhance model accuracy and applicability. By addressing these issues, the performance of the AI model in road condition assessment in practical applications can be improved to be more accurate and reliable.

In addition, the AI model in this study is based primarily on daytime or well-lit images of the roadway. The model would need additional work or specialized cameras to incorporate more nighttime images or poorly lit roadways.

## **6.0 IMPLEMENTATION AND RECOMMENDATIONS**

To implement the developed AI model in practice, future steps and required resources are as follows:

### **1. Deliverables:**

The deliverables of this project include the Python code for AI model training, testing, and application in practice, the image dataset used for training, the developed model for automated snow-cover condition assessment, and relevant documents that provide guidance on model usage.

### **2. Technology Deployment:**

Generally, a real-time data pipeline needs to be created, connecting CCTV feeds to the AI model and delivering results to relevant departments in UDOT. The pipeline should ensure seamless data transfer, processing, and reporting. Specifically, based on the requirements of UDOT, the screenshots (images) for real-time road conditions should be taken. Then, documents can be put in a folder, correspondingly changing the file path in `Model_Inference.ipynb` to the file path of the folder, then clicking execution of code to generate the report of real-time road conditions in different sections of roads recorded by the CCTV camera network.

### **3. Organizational Roles and Responsibilities:**

**Field Technicians:** Technicians are required to install and maintain cameras and networking equipment across selected road sections, ensuring continuous data feed and camera functionality.

**Operational Staff:** Personnel are needed to take screenshots of images for real-time road conditions, feed images into the algorithm and get the road condition assessment results, manage the integration of AI-generated reports into snow plow operations, coordinate interventions, and respond to weather-related warnings.

## REFERENCES

- Arya, D., Maeda, H., Kumar Ghosh, S., Toshniwal, D., Omata, H., Kashiyama, T., & Sekimoto, Y. (2020). Global Road Damage Detection: State-of-the-art Solutions. *2020 IEEE International Conference on Big Data (Big Data)*, 5533–5539. <https://doi.org/10.1109/BigData50022.2020.9377790>
- Brook, J. P., Protat, A., Soderholm, J. S., Warren, R. A., & McGowan, H. (2022). A Variational Interpolation Method for Gridding Weather Radar Data. *Journal of Atmospheric and Oceanic Technology*, 39(11), 1633–1654. <https://doi.org/10.1175/JTECH-D-22-0015.1>
- Carrillo, J., Crowley, M., Pan, G., & Fu, L. (n.d.). *Design of Efficient Deep Learning models for Determining Road Surface Condition from Roadside Camera Images and Weather Data*.
- Foehn, A., García Hernández, J., Schaepli, B., & De Cesare, G. (2018). Spatial interpolation of precipitation from multiple rain gauge networks and weather radar data for operational applications in Alpine catchments. *Journal of Hydrology*, 563, 1092–1110. <https://doi.org/10.1016/j.jhydrol.2018.05.027>
- Gong, Y., Zhan, Z., Jin, Q., Li, Y., Idelbayev, Y., Liu, X., Zharkov, A., Aberman, K., Tulyakov, S., Wang, Y., & Ren, J. (2024, January 11). *E<sup>2</sup>GAN: Efficient Training of Efficient GANs for Image-to-Image Translation*. arXiv.Org. <https://arxiv.org/abs/2401.06127v2>
- Goodfellow, I. J., Pouget-Abadie, J., Mirza, M., Xu, B., Warde-Farley, D., Ozair, S., Courville, A., & Bengio, Y. (2014). *Generative Adversarial Networks* (arXiv:1406.2661). arXiv. <https://doi.org/10.48550/arXiv.1406.2661>
- Huang, M. Q., Ninić, J., & Zhang, Q. B. (2021). BIM, machine learning and computer vision techniques in underground construction: Current status and future perspectives. *Tunnelling and Underground Space Technology*, 108, 103677. <https://doi.org/10.1016/j.tust.2020.103677>
- Kawai, S., Takeuchi, K., Shibata, K., & Horita, Y. (2014). A Smart Method to Distinguish Road Surface Conditions at Night-time using a Car-Mounted Camera. *IEEJ Transactions on Electronics, Information and Systems*, 134(6), 878–884. <https://doi.org/10.1541/ieejieiss.134.878>
- Khan, M. N., & Ahmed, M. M. (2021). Development of a Novel Convolutional Neural Network Architecture Named RoadweatherNet for Trajectory-Level Weather Detection using SHRP2 Naturalistic Driving Data. *Transportation Research Record: Journal of the*

- Transportation Research Board*, 2675(9), 1016–1030.  
<https://doi.org/10.1177/03611981211005470>
- Khan, M. N., & Ahmed, M. M. (2022). Weather and surface condition detection based on road-side webcams: Application of pre-trained Convolutional Neural Network. *International Journal of Transportation Science and Technology*, 11(3), 468–483.  
<https://doi.org/10.1016/j.ijst.2021.06.003>
- Koch, C., Georgieva, K., Kasireddy, V., Akinci, B., & Fieguth, P. (2015). A review on computer vision based defect detection and condition assessment of concrete and asphalt civil infrastructure. *Advanced Engineering Informatics*, 29(2), 196–210.  
<https://doi.org/10.1016/j.aei.2015.01.008>
- Krizhevsky, A., Sutskever, I., & Hinton, G. E. (2017). ImageNet classification with deep convolutional neural networks. *Communications of the ACM*, 60(6), 84–90.  
<https://doi.org/10.1145/3065386>
- Ledig, C., Theis, L., Huszar, F., Caballero, J., Cunningham, A., Acosta, A., Aitken, A., Tejani, A., Totz, J., Wang, Z., & Shi, W. (2016, September 15). *Photo-Realistic Single Image Super-Resolution Using a Generative Adversarial Network*. arXiv.Org.  
<https://arxiv.org/abs/1609.04802v5>
- Lepcha, D. C., Goyal, B., Dogra, A., & Goyal, V. (2023). Image super-resolution: A comprehensive review, recent trends, challenges and applications. *Information Fusion*, 91, 230–260. <https://doi.org/10.1016/j.inffus.2022.10.007>
- Lu, Y. (2019). Artificial intelligence: A survey on evolution, models, applications and future trends. *Journal of Management Analytics*, 6(1), 1–29.  
<https://doi.org/10.1080/23270012.2019.1570365>
- O’Mahony, N., Campbell, S., Carvalho, A., Harapanahalli, S., Hernandez, G. V., Krpalkova, L., Riordan, D., & Walsh, J. (2020). Deep Learning vs. Traditional Computer Vision. In K. Arai & S. Kapoor (Eds.), *Advances in Computer Vision* (Vol. 943, pp. 128–144). Springer International Publishing. [https://doi.org/10.1007/978-3-030-17795-9\\_10](https://doi.org/10.1007/978-3-030-17795-9_10)
- Oriol, B., & Miot, A. (2021, October 21). *On some theoretical limitations of Generative Adversarial Networks*. arXiv.Org. <https://arxiv.org/abs/2110.10915v1>
- Qian, Y., Almazan, E. J., & Elder, J. H. (2016). Evaluating features and classifiers for road weather condition analysis. *2016 IEEE International Conference on Image Processing (ICIP)*,

- 4403–4407. <https://doi.org/10.1109/ICIP.2016.7533192>
- Redmon, J., Divvala, S., Girshick, R., & Farhadi, A. (2016). You Only Look Once: Unified, Real-Time Object Detection. *2016 IEEE Conference on Computer Vision and Pattern Recognition (CVPR)*, 779–788. <https://doi.org/10.1109/CVPR.2016.91>
- Samo, M., Mafeni Mase, J. M., & Figueredo, G. (2023). Deep Learning with Attention Mechanisms for Road Weather Detection. *Sensors*, 23(2), 798. <https://doi.org/10.3390/s23020798>
- Sirirattanapol, C., Nagai, M., Witayangkurn, A., Pravinvongvuth, S., & Ekpanyapong, M. (2019). Bangkok CCTV Image through a Road Environment Extraction System Using Multi-Label Convolutional Neural Network Classification. *ISPRS International Journal of Geo-Information*, 8(3), 128. <https://doi.org/10.3390/ijgi8030128>
- Spencer, B. F., Hoskere, V., & Narazaki, Y. (2019). Advances in Computer Vision-Based Civil Infrastructure Inspection and Monitoring. *Engineering*, 5(2), 199–222. <https://doi.org/10.1016/j.eng.2018.11.030>
- Voulodimos, A., Doulamis, N., Doulamis, A., & Protopapadakis, E. (2018). Deep Learning for Computer Vision: A Brief Review. *Computational Intelligence and Neuroscience*, 2018, e7068349. <https://doi.org/10.1155/2018/7068349>
- Wilson, A. M., & Silander, J. A. (2014). Estimating uncertainty in daily weather interpolations: A Bayesian framework for developing climate surfaces: UNCERTAINTY IN DAILY WEATHER INTERPOLATIONS. *International Journal of Climatology*, 34(8), 2573–2584. <https://doi.org/10.1002/joc.3859>
- Zhao, B., Li, X., Lu, X., & Wang, Z. (2018). A CNN–RNN architecture for multi-label weather recognition. *Neurocomputing*, 322, 47–57. <https://doi.org/10.1016/j.neucom.2018.09.048>